Communications to SIMAI Congress,
ISSN 1827-9015, Vol. 1 (2006)
DOI: 10.1685/CSC06064

Plane-wave expansion of the electromagnetic Green-function for translating sources inside a rectangular waveguide with dissipative walls

Peter De Cupis, Giorgio Gerosa
Dipartimento. di Ingegneria Elettronica, Università di Roma La Sapienza, via Eudossiana 18, 00184 Roma, Italy

INTRODUCTION

The Special Relativity, with its inherent axioms on space-time relations between inertial frames, provides the exact theoretical toolkit for studying Electro-Magnetic (EM) radiation/diffraction by uniformly translating sources/scatterers, i.e. the so-called "Frame Hopping Method" (FHM) [1]: in the case of point, the EM emission/diffraction is firstly evaluated in the reference frame where the source/scatterer appears at rest (co-moving frame); secondly, Einstein covariance relations are applied to the EM field expression in order to recast it in the form that is relevant to the actual observer reference frame (laboratory frame).

In the free-space geometry the FHM allows us to immediately generalize the motionless solution of any radiation/diffraction problem to the relativistic case [1]; on the other hand, in bounded geometries, i.e. in the presence of additional confining surfaces, the application of the FHM becomes delicate: as a matter of fact, in the co-moving frame the EM problem is not motionless, because of the relative translation between the source/scatterer and the confining surfaces; therefore, the customary motionless boundary conditions can not be employed. For instance, in the problem under examination, i.e. the radiation by an EM source that translates in the axial direction inside a rectangular wave-guide, the backward translation of the walls, that is experienced in the antenna rest frame, forbids a straightforward generalization of the standard modal expansion of the motionless EM Green function: in fact, the wave-guide modes are found by solving an eigenvalue problem for the Helmholtz operator acting on the functional space over the transverse section that is defined by rightly associate boundary conditions [2]; for shifting walls the standard Dirichlet and Neumann conditions relevant to Transverse Magnetic (TM) and Transverse Electric (TE) modes, respectively, become no more consistent, whilst rather intricate moving-boundary conditions [3] should be introduced for correctly defining the transverse functional space.

The employed formulation avoids the TE/TM modal expansion and the subsequent relativistic complication of the boundary conditions. In the case of point, the EM Green function (expressing the radiation by an arbitrarily oriented Hertz dipole) shall be directly set in the form of a Plane-Wave (PW) spectrum, so that the relative motion of the boundary walls can be taken into account in terms of some simple adjustments to the customary Fresnel laws relevant to the PW reflection from a motionless plane interface: in fact, the parallel boundary translation causes no Doppler frequency shift between the incident and the reflected waves; also, the usual Snell equality for incidence and reflection angles is maintained in the moving frame; the PW reflection coefficients can be evaluated by means of the usual Fresnel rule relevant to the motionless case, provided that the values of the incident angles and frequency, as recorded in the frame where the interface appears at rest, are employed [1,4-7]. Furthermore, relativistic transformations for the PW parameters (angles, frequency, polarization coefficients) have a very simple analytic expression; correspondingly, the PW spectral expansion of the EM Green function can be covariance transformed between the involved frames with minimal algebra [4-7].

FORMULATION

Let us consider an axially infinite wave-guide, with rectangular transverse section, bounded by homogeneous dissipative walls. A radiating Hertz-dipole and the signal observer are assumed to be both translating in the inner vacuum volume along the axial direction $\hat{\mathbf{x}}_3$. At the outset we distinguish three reference frames: Σ', where the radiating dipole appears at rest; Σ_1, where the observer appears at rest; and Σ_2, which is the wave-guide rest frame. The relative velocities of the Hertz-dipole with respect to the receiver and the wave-guide are assumed to be $\beta_1 c\hat{\mathbf{x}}_3$ and $\beta_2 c\hat{\mathbf{x}}_3$, respectively, where c is the speed of light *in vacuo* (correspondingly, $(\beta_2 - \beta_1)c\hat{\mathbf{x}}_3$ is the relative speed of the translating receiver with respect to the guide).

Licensed under the Creative Commons Attribution Noncommercial No Derivatives

In the dipole rest frame Σ' we assume that the radiated e.m. field is represented by means of a PW integral expansion on the real two-dimensional spectral variable $\boldsymbol{\eta}=[\chi,\zeta]$, plus a Dirac δ-term which shall take into account the EM field singularity at the impulsive source point $[x'^1, x'^2, x'^3]=\boldsymbol{\Xi}=[\Xi^1, \Xi^2, 0]$, see Fig.1: in fact, we let (Einstein's convention for summation on the repeated indexes $p, y \in \{1,2\}$; $\boldsymbol{\xi}=[\xi_1,\xi_2] \in \{1,2\}^2$; $r \in \{1,2,3\}$; $a \in \{0,1,2,3\}$ is adopted):

$$\bar{\mathrm{F}}'^{hl}\left(\tilde{\mathrm{X}}'\right)=I'^{y}\alpha'^{ry}\left\{g'^{hl}_{ry}\delta\left(x'^1-\Xi^1\right)\,\delta\left(x'^2-\Xi^2\right)\delta\left(x'^3\right)+\right.$$

$$\left.+\int_{-\infty}^{+\infty}\int_{-\infty}^{+\infty}\Psi^{phl}\left(\theta'_{\xi}(\boldsymbol{\eta}),\,\phi'_{\xi}(\boldsymbol{\eta})\right)\exp\left[i\tilde{x}'^{a}\tilde{K}_a\left(\omega',\,\theta'_{\xi}(\boldsymbol{\eta}),\,\phi'_{\xi}(\boldsymbol{\eta})\right)\right]\mathrm{A}'^{\xi}_{pry}(x'^1,x'^2;\boldsymbol{\eta})d\boldsymbol{\eta}\right\}\ ,\ h=1,2;\ l=1-3\ ; \quad (1)$$

$$\mathrm{Re}\left\{\bar{\mathrm{F}}'^{1l}\left(\tilde{\mathrm{X}}'\right),\bar{\mathrm{F}}'^{2l}\left(\tilde{\mathrm{X}}'\right)\right\}=\left\{\boldsymbol{E}'\left(\tilde{\mathrm{X}}'\right),Z\boldsymbol{H}'\left(\tilde{\mathrm{X}}'\right)\right\}\bullet\hat{\mathbf{x}}_l\ ,\ l=1-3 \qquad ; \quad (2)$$

$\boldsymbol{E}'\left(\tilde{\mathrm{X}}\right)$ and $\boldsymbol{H}'\left(\tilde{\mathrm{X}}'\right)$ are the electric field and the magnetic field, respectively, as measured at the space-time position $\tilde{\mathrm{X}}'=\left\|\tilde{x}'^{a}\right\|_{a=0-3}=\left[ct',x'^1,x'^2,x'^3\right]$; $c=1/\sqrt{\varepsilon_0\mu_0}$; $Z=\sqrt{\mu_0/\varepsilon_0}$; $i=+\sqrt{-1}$; $\hat{\mathbf{x}}_1,\hat{\mathbf{x}}_2,\hat{\mathbf{x}}_3$ are the Cartesian unit vectors; $\omega'=2\pi c/\lambda'$, I'^{y}, $\hat{\boldsymbol{\alpha}}'^{y}=\alpha'^{ay}\hat{\mathbf{x}}_a$ are the (circular) frequency, the peak amplitude, and the direction of the electric (y=1) and magnetic (y=2) source currents, respectively, as experienced in Σ';. the propagation direction of each PW component is determined by means of the zenithal and azimuthal angles $\theta'_{\xi}(\boldsymbol{\eta}),\phi'_{\xi}(\boldsymbol{\eta})$ defined as follows (uniform PWs for $\zeta^2+\chi^2\le 1$, evanescent PWs for $\zeta^2+\chi^2>1$):

$$\cos\theta'_{\xi}(\boldsymbol{\eta})=\chi\ \ ;\ \sin\theta'_{\xi}(\boldsymbol{\eta})=(-1)^{\xi_1}\left(1-\chi^2\right)^{1/2}\ ;\quad \xi_1,\xi_2=1,2 \quad (3)$$

$$\cos\phi'_{\xi}(\boldsymbol{\eta})=\left(1-\zeta^2-\chi^2\right)^{1/2}\ \left(1-\chi^2\right)^{-1/2},\ \sin\phi'_{\xi}(\boldsymbol{\eta})=(-1)^{\xi_2-\xi_1}\left|\zeta\right|\left(1-\chi^2\right)^{-1/2}\ ;\quad \xi_1,\xi_2=1,2\ . \quad (4)$$

For a plane-wave, propagating *in vacuo*, characterized by circular frequency ϖ, zenith τ and azimuth φ, we defined the following symbols:

$$\left\|\tilde{K}_a\left(\omega,\tau,\varphi\right)\right\|_{a=0-3}=c^{-1}\omega\left[-1,\sin\tau\cos\varphi,\sin\tau\sin\varphi,\cos\tau\right] \quad (5)$$

$$\left\|\Psi^{1hl}\left(\tau,\varphi\right)\right\|_{l=1-3}^{h=1,2}=\begin{bmatrix}\cos\tau\cos\varphi & \cos\tau\sin\varphi & -\sin\tau\\ -\sin\varphi & \cos\varphi & 0\end{bmatrix};\left\|\Psi^{2hl}\left(\tau,\varphi\right)\right\|_{l=1-3}^{h=1,2}=\begin{bmatrix}-\sin\varphi & \cos\varphi & 0\\ -\cos\tau\cos\varphi & -\cos\tau\sin\varphi & \sin\tau\end{bmatrix}. \quad (6)$$

From Eqs. (3)-(5) we observe[1] that the PW indexes $\xi_n=1$ and $\xi_n=2$ refer to regressive ($\partial_{x'^m}[\arg\bar{\mathrm{F}}^{hl}]<0$) and progressive ($\partial_{x'^m}[\arg\bar{\mathrm{F}}^{hl}]>0$) propagation, respectively, with respect to the $\hat{\mathbf{x}}_n$ axis, for $n=1,2$. On the other hand, from Eq. (6) we note that the PW binary index p=1,2 distinguishes the two kinds of linear sub-polarizations, whereinto the generic elliptical polarization can be decomposed [6,7]. We also assume that the PW integral expansion for the continuous part of the radiated field given in Eq. (1) has a peculiar, local form in any one of the four quadrants [i.e. $Q_1=\left(0,\Xi^1\right)\times\left(0,\Xi^2\right)$, $Q_2=\left(\Xi^1,\Delta^1\right)\times\left(0,\Xi^2\right)$, $Q_3=\left(\Xi^1,\Delta^1\right)\times\left(\Xi^2,\Delta^2\right)$, $Q_4=\left(0,\Xi^1\right)\times\left(\Xi^2,\Delta^2\right)$] which decompose the rectangular section, taking the source point as a pole, see Fig.1: correspondingly, for the PW spectral amplitude coefficients in Eq. (1), we let:

$$\mathrm{A}'^{\xi}_{pry}(x'^1,x'^2;\boldsymbol{\eta})\equiv B'^{\xi}_{jpry}(\boldsymbol{\eta})\ \forall\left(x'^1,x'^2\right)\in Q_j\ \ ,\ \xi_1,\xi_2,p,y=1,2;\ r=1-3\qquad , \quad (7)$$

Any PW component, defined through Eqs. (3)-(7), individually verifies the source-less Maxwell equations, which are valid for $x'^{r}\hat{\mathbf{x}}_r\neq\boldsymbol{\Xi}$. Then, on any one of the four guide walls (i.e. $\mathrm{W}_1=\left\{x'^1\equiv\Delta^1\right\}$; $\mathrm{W}_2=\left\{x'^2\equiv\Delta^2\right\}$, $\mathrm{W}_3=\left\{x'^1\equiv 0\right\}$, $\mathrm{W}_4=\left\{x'^2\equiv 0\right\}$), the integral sum in Eq. (1) shall globally verify the boundary condition; this can be achieved because PW spectral components can be classified in incident and reflected components, according to the propagation features stated by Eqs. (3), (4). In the case of point, at any wall W_m, $m=1-4$, we can distinguish '*mirroring* couples' of incident and reflected PWs, where a mirroring couple is characterized by the same value of the

[1] In fact, we get: $\tilde{x}'^{a}\tilde{K}_a\left(\omega',\,\theta'_{\xi}(\boldsymbol{\eta}),\,\phi'_{\xi}(\boldsymbol{\eta})\right)=c^{-1}\omega'\{[x'^3\chi+(-1)^{\xi_1}x'^1\left(1-\zeta^2-\chi^2\right)^{1/2}+(-1)^{\xi_2}\left|\zeta\right|x'^2]-ct'\}$

spectral variable $\boldsymbol{\eta}$, and complementary values of the directional index ξ, as specified below:

	incident index	reflected index	Fresnel reflection conditions (for $p, y = 1,2;\ r = 1-3$)
W_1	$\xi_1 = 2$	$\xi_1 = 1$	$B'^{(1,\xi_2)}_{jpry}(\boldsymbol{\eta}) = \Lambda_1^+(\boldsymbol{\eta})\sum_{b=1}^{2}\ \Gamma^b_{1p}\left(\omega_2(\boldsymbol{\eta}), \theta^2_{(2,\xi_2)}(\boldsymbol{\eta}), \phi^2_{(2,\xi_2)}(\boldsymbol{\eta}) + \pi\right) B'^{(2,\xi_2)}_{jbry}(\boldsymbol{\eta}),\ \xi_2 = 1,2;\ j = 2,3$
W_2	$\xi_2 = 2$	$\xi_2 = 1$	$B'^{(\xi_1,1)}_{jpry}(\boldsymbol{\eta}) = \Lambda_2^+(\boldsymbol{\eta})\sum_{b=1}^{2}\ \Gamma^b_{2p}\left(\omega_2(\boldsymbol{\eta}), \theta^2_{(\xi_1,2)}(\boldsymbol{\eta}), \phi^2_{(\xi_1,2)}(\boldsymbol{\eta}) + \frac{\pi}{2}\right) B'^{(\xi_1,2)}_{jbry}(\boldsymbol{\eta}),\ \xi_1 = 1,2;\ j = 3,4$
W_3	$\xi_1 = 1$	$\xi_1 = 2$	$B'^{(2,\xi_2)}_{jpry}(\boldsymbol{\eta}) = \Lambda_1^-(\boldsymbol{\eta})\sum_{b=1}^{2}\ \Gamma^b_{3p}\left(\omega_2(\boldsymbol{\eta}), \theta^2_{(1,\xi_2)}(\boldsymbol{\eta}), \phi^2_{(1,\xi_2)}(\boldsymbol{\eta})\right) B'^{(1,\xi_2)}_{jbry}(\boldsymbol{\eta}),\ \xi_2 = 1,2;\ j = 1,4$
W_4	$\xi_2 = 1$	$\xi_2 = 2$	$B'^{(\xi_1,2)}_{jpry}(\boldsymbol{\eta}) = \Lambda_2^-(\boldsymbol{\eta})\sum_{b=1}^{2}\ \Gamma^b_{4p}\left(\omega_2(\boldsymbol{\eta}), \theta^2_{(\xi_1,1)}(\boldsymbol{\eta}), \phi^2_{(\xi_1,1)}(\boldsymbol{\eta}) - \frac{\pi}{2}\right) B'^{(\xi_1,1)}_{jbry}(\boldsymbol{\eta}),\ \xi_1 = 1,2;\ j = 1,2$

By virtue of Eqs. (3), (4) any mirroring couple intrinsically verify Snell laws. Then, the Fresnel laws relating amplitude coefficients must be imposed; the alteration due to the shift of the walls (which is experienced in frame Σ') can be simply expressed 'feeding' the customary motionless formulas for Fresnel coefficients by modified values of the incident wave parameters, i.e. by frequency, zenith and azimuth as measured in the guide rest frame Σ_2 (see Refs.[1,4-7]), as it is stated in the last column of the table, where: $\Gamma^b_{mp}(\omega, \tau, \varphi)$, ($m = 1-4$; b,p=1,2) are the customary motionless Fresnel coefficients relevant to the wall W_m (incident PW frequency ω, zenith τ and azimuth φ), furnishing the *c*-th reflected sub-polarization that originates from the *b*-th incident sub-polarization; $\Lambda^{\pm}_n(\boldsymbol{\eta})$, *n*=1,2, are factors expressing the phase displacement between progressive and regressive mirroring terms at the various interfaces, i.e. from Eqs. (3)-(5):

$$\Lambda_1^{\pm}(\boldsymbol{\eta}) = \exp\left[\pm ic^{-1}\omega'\left[2\Delta^1\left(1-\zeta^2-\chi^2\right)^{1/2}\right]\right], \qquad \Lambda_2^{\pm}(\boldsymbol{\eta}) = \exp\left[\pm ic^{-1}\omega'\left(2\Delta^2|\zeta|\right)\right] \quad ; \tag{8}$$

frequency and angular parameters of the PW components, as recorded in frames $\sum_{\upsilon}$, υ=1,2, can be obtained through the following formulas, see Refs. [4-7] (let $\gamma_{\upsilon} = [1+(\beta_{\upsilon})^2]^{-1/2}$):

$$\omega_{\upsilon}(\boldsymbol{\eta}) = \gamma_{\upsilon}\left(1+\beta_{\upsilon}\cos\theta'_{\xi}(\boldsymbol{\eta})\right)\omega' = \gamma_{\upsilon}\left(1+\beta_{\upsilon}\chi\right)\omega' \qquad ,\ \upsilon = 1,2 \tag{9}$$

$$\cos\theta^{\upsilon}_{\xi}(\boldsymbol{\eta}) = \frac{\cos\theta'_{\xi}(\boldsymbol{\eta})+\beta_{\upsilon}}{1+\beta_{\upsilon}\cos\theta'_{\xi}(\boldsymbol{\eta})}\ ,\ \sin\theta^{\upsilon}_{\xi}(\boldsymbol{\eta}) = \frac{\sin\theta'_{\xi}(\boldsymbol{\eta})}{\gamma_{\upsilon}\left(1+\beta_{\upsilon}\cos\theta'_{\xi}(\boldsymbol{\eta})\right)}\ ;\ \phi^{\upsilon}_{\xi}(\boldsymbol{\eta}) = \phi'_{\xi}(\boldsymbol{\eta})\ ;\quad \xi_1,\xi_2,\upsilon = 1,2 \tag{10}$$

A complete algebraic system for computing the unknown PW spectral amplitude coefficients $B'^{\xi}_{jpry}(\boldsymbol{\eta})$, $\xi_1,\xi_2,p,y = 1,2;\ r = 1-3;\ j = 1-4$, can be achieved by joining the above-displayed Fresnel constraints, with the conditions which can be obtained by imposing the continuity of the different 'local' PW spectra, relevant to adjacent quadrants, at their mutual boundaries, i.e. for $x'^1 \equiv \Xi^1$ and $x'^2 \equiv \Xi^2$; at once, it is necessary to consider the Dirac source term for $\left[x'^1, x'^2\right] = \left[\Xi^1, \Xi^2\right]$, i.e.:

$$\delta\left(x'^1-\Xi^1\right)\ \delta\left(x'^2-\Xi^2\right)\delta\left(x'^3\right) = \frac{\delta\left(x'^1-\Xi^1\right)}{\left(2\pi\right)^2}\int_{-\infty}^{+\infty}\int_{-\infty}^{+\infty}\exp\left[-i\Xi^2\zeta\right]\exp\left[i\left(x'^2\zeta+x'^3\chi\right)\right]d\zeta d\chi \qquad , \tag{11}$$

so that the amplitude coefficients $\{g'^{hl}_{ry}\}_{h,y=1,2;\ l,r=1-3}$ of the supplementary impulsive EM field term can be contemporarily evaluated, cfr. Refs. [6,7]; in fact, if all such conditions are verified, the validity of the solution proposed in Eq. (1) is granted by virtue of the Uniqueness Theorem.

Finally, the expression of the EM field, as actually experienced in the receiver rest frame Σ_1, i.e. $\left\{\boldsymbol{E}\left(\tilde{\mathrm{X}}\right), \boldsymbol{H}\left(\tilde{\mathrm{X}}\right)\right\} = \left\{F^{1l}\left(\tilde{\mathrm{X}}\right), Z^{-1}\overline{F}^{2l}\left(\tilde{\mathrm{X}}\right)\right\}\hat{\mathbf{x}}_l = \mathrm{Re}\left\{\overline{\mathrm{F}}^{1l}\left(\tilde{\mathrm{X}}\right), Z^{-1}\overline{\mathrm{F}}^{2l}\left(\tilde{\mathrm{X}}\right)\right\}\hat{\mathbf{x}}_l$, at the Lorentz-transformed space-time abscissa $\tilde{\mathrm{X}} = \left\|\tilde{x}^a\right\|_{a=0-3} = \left[ct, x^1, x^2, x^3\right] = \left[\gamma_1\left(ct'+\beta_1 x'^3\right), x'^1, x'^2, \gamma_1\left(x'^3+\beta_1 ct'\right)\right]$, is obtained by applying the $\Sigma' \rightarrow \Sigma_1$ relativistic covariance transformations to Eq. (1); for $\left[x^1, x^2\right] = \left[x'^1, x'^2\right] \neq \left[\Xi^1, \Xi^2\right]$ we get:

$$\overline{\mathrm{F}}^{hl}\left(\tilde{\mathrm{X}}\right) = I'^{y}\alpha'^{ry}\int_{-\infty}^{+\infty}\int_{-\infty}^{+\infty}\Psi^{phl}\left(\theta^1_{\xi}(\boldsymbol{\eta}),\ \phi^1_{\xi}(\boldsymbol{\eta})\right)\exp\left[i\tilde{x}^a\tilde{K}_a\left(\omega_1(\boldsymbol{\eta}),\ \theta^1_{\xi}(\boldsymbol{\eta}),\ \phi^1_{\xi}(\boldsymbol{\eta})\right)\right]\mathrm{A}^{\xi}_{pry}(x^1, x^2; \boldsymbol{\eta})d\boldsymbol{\eta}\ ,\ {}^{l=1-3}_{h=1,2}, \tag{12}$$

with un-primed PW frequency and angles given by Eqs. (9)-(10), and, see Refs. [4-7]:

$$\mathrm{A}^{\xi}_{pry}(x^1,x^2;\boldsymbol{\eta}) = \gamma_1\left(1+\beta_1\cos\theta'_{\xi}\ (\boldsymbol{\eta})\right)\mathrm{A}'^{\xi}_{pry}(x^1,x^2;\boldsymbol{\eta}) = \gamma_1\left(1+\beta_1\chi\right)\mathrm{A}'^{\xi}_{pry}(x'^1,x'^2;\boldsymbol{\eta})\ ,\ \xi_1,\xi_2,p=1,2;\ r=1\text{-}3 \quad (13)$$

The expression (12) represents a multi-chromatic PW spectrum; in fact, at a fixed position $\mathrm{X}=[x^1,x^2,x^3]$, its dependence on time t can be explicitly recast as follows, see Eq. (9):

$$F^{hl}_{\mathrm{X}}(t) = \overset{\mathrm{Re}}{\overline{\mathrm{F}}}{}^{hl}_{\mathrm{X}}(t) \doteq \mathrm{Re}\left[\overline{\mathrm{F}}^{hl}\left([\mathrm{X},ct]\right)\right] = \overset{\mathrm{Re}}{\int_{-\infty}^{+\infty}} T^{hl}_{\mathrm{X}}(\chi)\exp\left[-i\omega'\gamma_1\left(1+\beta_1\chi\right)t\right]d\chi\ ,\ {}^{l=1-3}_{h=1,2} \quad (14)$$

Long-term (i.e. for an observation time-window $dt \gg 1/\omega'$) measurements by a spectrum analyser can be represented by means of the Fourier frequency transform to the variable Ω, i.e.:

$$\Im\left[F^{hl}_{\mathrm{X}},\Omega\right] = \int_{-\infty}^{+\infty} F^{hl}_{\mathrm{X}}(t)\exp\left[i\Omega t\right]dt\ ,\ {}^{l=1-3}_{h=1,2} \quad , \quad (15)$$

Such transform (named Doppler frequency spectrum) can be evaluated in the following closed-form expression (see Refs.[4]-[7]):

$$\Im\left[F^{hl}_{\mathrm{X}},\Omega\right] = \tfrac{1}{2}\left(\Im\left[\overline{\mathrm{F}}^{hl}_{\mathrm{X}},\Omega\right] + \left[\Im\left[\overline{\mathrm{F}}^{hl}_{\mathrm{X}},-\Omega\right]\right]^{*}\right), \Im\left[\overline{\mathrm{F}}^{hl}_{\mathrm{X}},\Omega\right] = \int_{-\infty}^{+\infty}\overline{\mathrm{F}}^{hl}_{\mathrm{X}}(t)\exp\left[i\Omega t\right]dt = \frac{T^{hl}_{\mathrm{X}}\left(\beta_1^{-1}\left(\gamma_1^{-1}\Omega/\omega'-1\right)\right)}{\beta_1\gamma_1\omega'}\ ,\ {}^{l=1-3}_{h=1,2} \quad (16)$$

On the other hand, direct time-domain signal analysis on a short observation window scale can be performed by evaluating the instantaneous amplitude and frequency modulations, with respect to the nominal emitting frequency ω': they correspond to the amplitude $\mathrm{M}^{hl}_{\mathrm{X};\omega'}(t) = \left|\mathbb{F}^{hl}_{\mathrm{X};\omega'}(t)\right|$ and to the argument sign-reversal time-derivative $f^{hl}_{\mathrm{X};\omega'}(t) = -\partial_t\left[\mathrm{Arg}\left[\mathbb{F}^{hl}_{\mathrm{X};\omega'}(t)\right]\right]$ of the complex envelope $\mathbb{F}^{hl}_{\mathrm{X};\omega'}(t)$, respectively, that is defined as follows:

$$\begin{bmatrix}\mathrm{Re}\left[\mathbb{F}^{hl}_{\mathrm{X};\omega'}(t)\right]\\ \mathrm{Im}\left[\mathbb{F}^{hl}_{\mathrm{X};\omega'}(t)\right]\end{bmatrix} = \begin{bmatrix}\cos\omega' t & \sin\omega' t\\ -\sin\omega' t & \cos\omega' t\end{bmatrix}\begin{bmatrix}F^{hl}_{\mathrm{X}}(t)\\ \breve{F}^{hl}_{\mathrm{X}}(t)\end{bmatrix},\ \breve{F}^{hl}_{\mathrm{X}}(t) = \lim_{\delta\to 0}\left(\int_{-\infty}^{t-\delta}+\int_{t-\delta}^{+\infty}\right)\left[\frac{F^{hl}_{\mathrm{X}}(\hat{t})}{\pi\left(t-\hat{t}\right)}d\hat{t}\right]\ ,\ {}^{l=1-3}_{h=1,2} \quad (17)$$

RESULTS

Aiming at investigating peculiarities of the Doppler phenomenology caused by the confining wave-guide walls, we applied Eqs. (14)-(17) in order to simulate a wide range of radiation experiments with assorted values of the physical and geometrical parameters. Figures 2,3 report results relevant to the Doppler frequency spectra: as like as in open-space experiments the band-with is generally dependent only on the relative velocity; on the other hand, the spatial confinement affects the spectral shape, generating a plurality of in-band spectral peaks: these are plausibly associated to the resonant eigen-modes of the guide [2], which are excited by the source. Time domain signal analysis, relevant to the instantaneous amplitude and frequency modulations, is shown in Figs. 4 and 5, respectively: as one can see, the amplitude is affected by ripple oscillations, which are likely due to the wall reflection, i.e. to the interference between the various excited modes; an analogous spurious undulation phenomenon, due to multi-modal interference, affects the instantaneous frequency modulation diagrams.

References

1. J. Van Bladel, *Relativity and Engineering* (Springer-Verlag, New York, 1984).
2. R.E. Collin, "Field Theory of guided waves" (IEEE Press, New York, 1991).
3. R.C. Costen, D. Adamson, "Three-dimensional derivation of the electrodynamic jump conditions and momentum-energy laws at a moving boundary," *Proc. IEEE*, vol. 53, no. 9, Sept. 1965.
4. P. De Cupis, "Radiation by a moving wire-antenna in the presence of a plane interface," Journal of Electromagnetic Waves and Applications, vol. 14 (2000), 1119-11132.
5. P. De Cupis, G. Gerosa and G. Schettini, "Electromagnetic scattering by uniformly moving bodies," Journal of Electromagnetic Waves and Applications, Vol. 14, no. 8, pp. 1037-1062, Aug. 2000.
6. P. De Cupis, "Plane-Wave spectra technique for the solution of EM radiation and scattering problems in moving media," Ph.D. Thesis, 'La Sapienza' University of Rome.
7. P. De Cupis, "Doppler-effect disturbance on the signal transmission between RF or μ-wave devices in relative motion on the earth surface," Abstract SPEEDAM 2002, 11-14 June 2002, Ravello (Italy), Abstract C2 25-29.

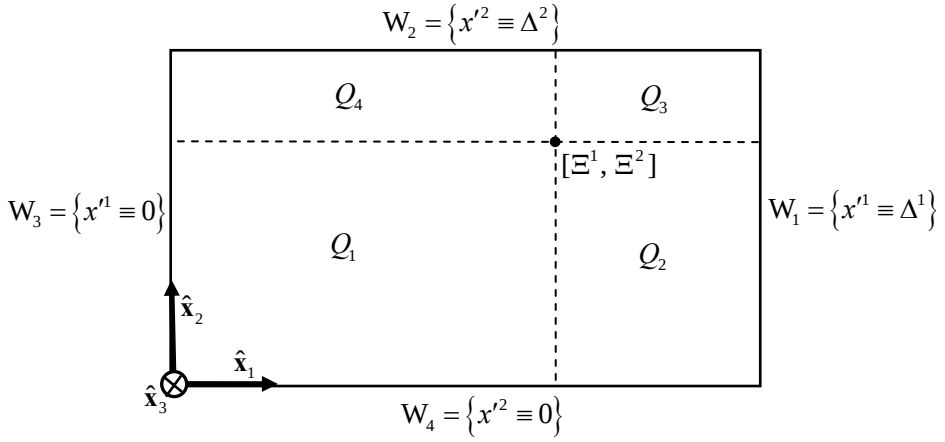


Fig.1 The transverse section of the wave-guide**.**

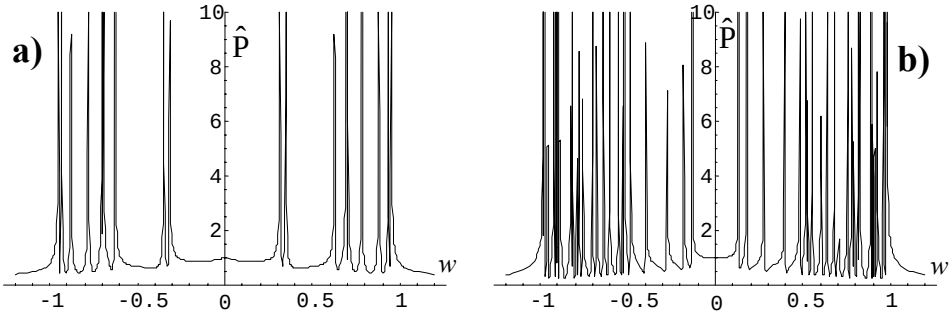


Fig.2 Normalized spectral amplitude $\hat{\mathrm{P}}(\Omega) = \|\mathbf{P}(\Omega)\| / \|\mathbf{P}(\omega')\|$ of the radiated Poynting vector $\mathbf{P} = \frac{1}{2}\Im[\boldsymbol{E}] \times (\Im[\boldsymbol{H}])^*$ vs. normalized frequency shift $w = (\Omega/\omega') - 1$. Simulation parameters: $\beta = \beta_1 = \beta_2 = 10^{-5}$; $\mathrm{X} = \left[x^1, x^2, x^3\right] = \left[0.75\Delta^1, 0.25\Delta^2, 0\right]$; $\left\{\Xi^1, \Xi^2\right\} = \left\{0.2\Delta^1, 0.7\Delta^2\right\}$; $\{\alpha'^{1y}, \alpha'^{2y}, \alpha'^{3y}\} = \left\{1, (-1)^y, 1\right\} / 3^{1/2}$, y=1,2;. $I'^1 = I'^2$. Guide with cement walls W_m, m=1–4; $\omega' = 1GHz$. Multi-modal emission: **a)** $\left\{\Delta^1, \Delta^2\right\} = \left\{1.6, 1.4\right\}\lambda'$; **b)** $\left\{\Delta^1, \Delta^2\right\} = \left\{2.6, 3.4\right\}\lambda'$.

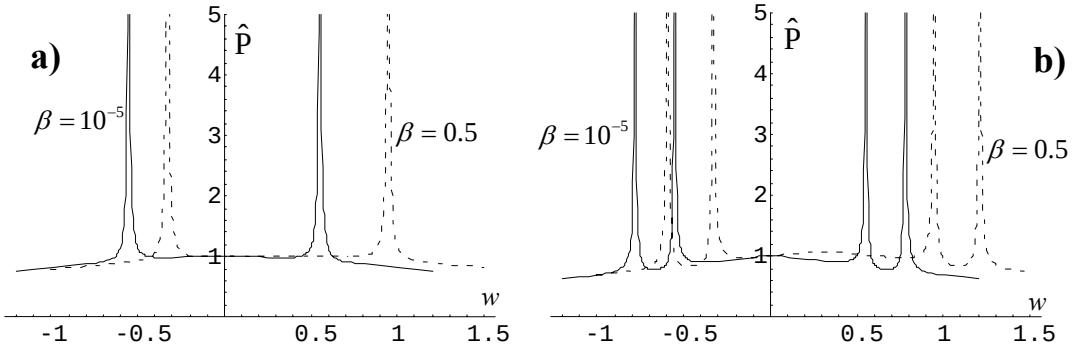


Fig.3 The same as fig. 2 for the synopsis of spectral diagrams relevant to $\beta = 10^{-5}$ (continuous line plots) and $\beta = 0.5$ (dotted line plots) **a)**. Single-modal emission, $\left\{\Delta^1, \Delta^2\right\} = \left\{0.4, 0.6\right\}\lambda'$. **b)** Double-modal emission, $\left\{\Delta^1, \Delta^2\right\} = \left\{0.6, 0.8\right\}\lambda'$

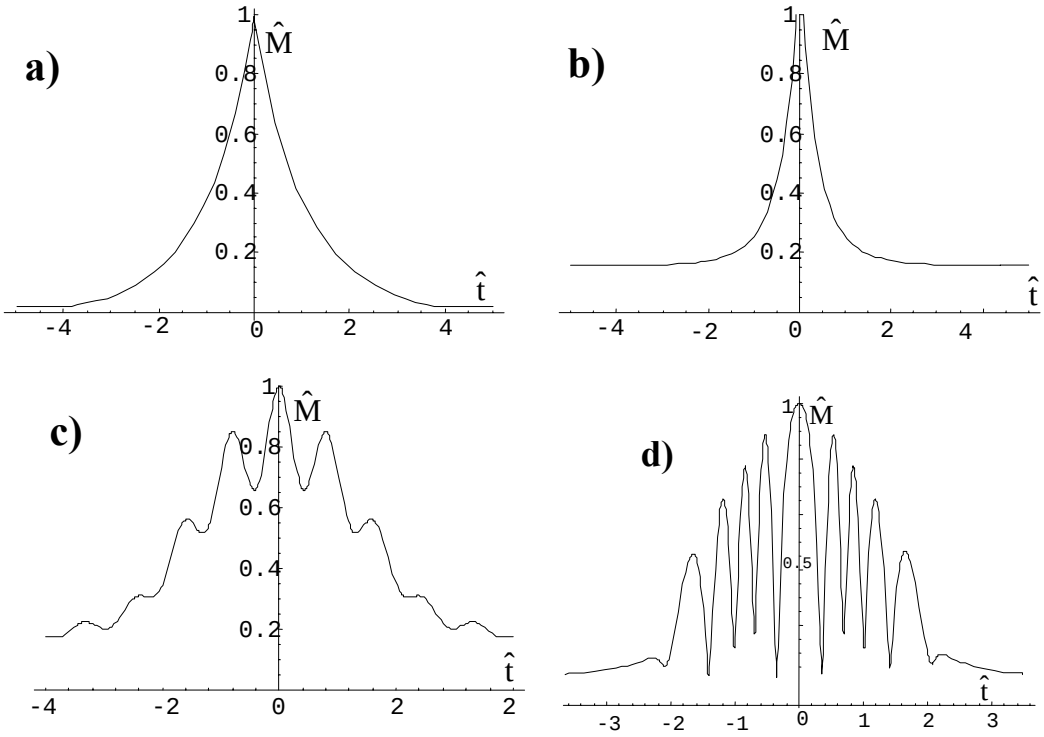


Fig.4 Normalized amplitude modulation for the $\hat{\mathbf{x}}$ component of the magnetic field ***H***, i.e. $\hat{\mathrm{M}}(t)=\mathrm{M}^{hl}_{\mathrm{X};\omega'}(t)/\mathrm{M}^{hl}_{\mathrm{X};\omega'}(0)$ for h=2, l=1, vs. normalized time $\hat{\mathrm{t}}=\beta t\omega'/2\pi$. Relative velocity: $\beta=10^{-5}$. All other experimental conditions are those of Fig. 2, except for: **a)** 0-modal emission, $\{\Delta^1,\Delta^2\}=\{0.4,0.3\}\lambda'$. **b)** Single-modal emission, $\{\Delta^1,\Delta^2\}=\{0.4,0.6\}\lambda'$ **c)** Double-modal emission, $\{\Delta^1,\Delta^2\}=\{0.6,0.8\}\lambda'$ **d)** Multi-modal emission, $\{\Delta^1,\Delta^2\}=\{3.6,2.8\}\lambda'$

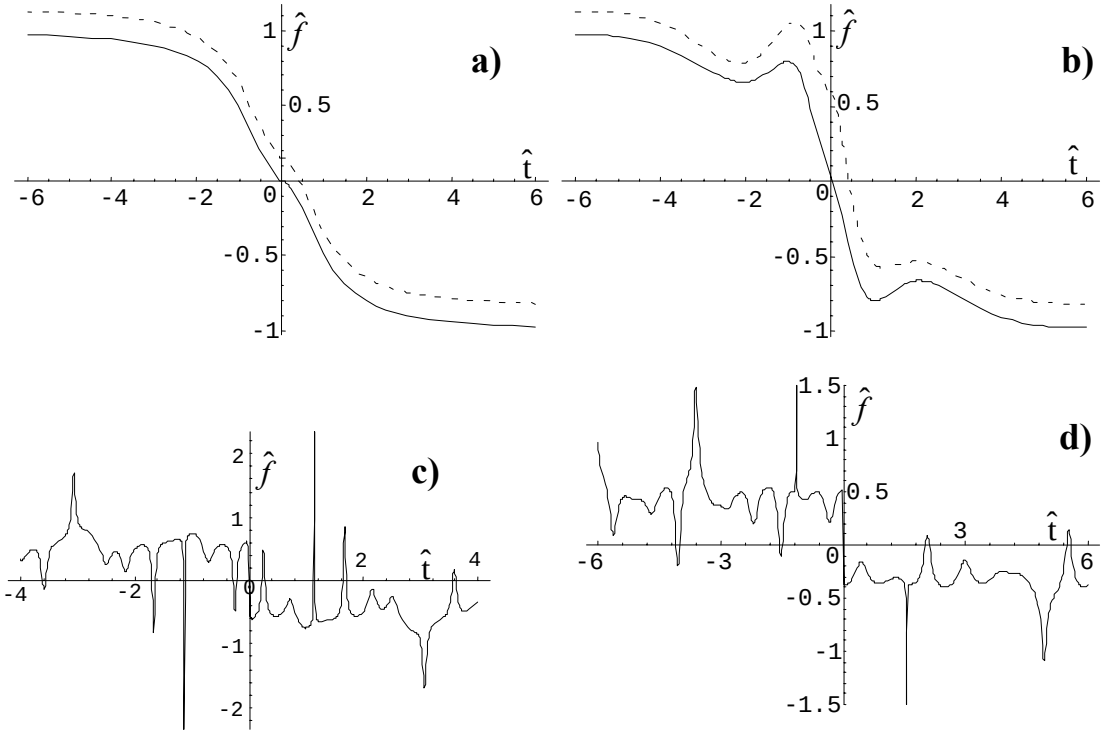


Fig.5 Normalized frequency shift for the $\hat{\mathbf{z}}$ component of the electric field ***E***, i.e. $\hat{f}(t)=(2\pi/\beta\omega')\cdot\{f^{hl}_{\mathrm{X};\omega'}(t)-\omega'/2\pi\}$ for h=1, l=3 , vs. normalized time $\hat{\mathrm{t}}=\beta t\omega'/2\pi$. **a)** Synopsis for $\beta=10^{-5}$ (continuous line plot) and $\beta=0.5$ (dotted line plot) in a single-mode emission case, $\{\Delta^1,\Delta^2\}=\{0.4,0.6\}\lambda'$ **b)** The same as a) for a double-modal emission, $\{\Delta^1,\Delta^2\}=\{0.6,0.8\}\lambda'$. **c)** Multi-modal emission, $\{\Delta^1,\Delta^2\}=\{2.9,3.3\}\lambda'$, for $\beta=10^{-5}$. **d)** Multi-modal emission, $\{\Delta^1,\Delta^2\}=\{2.1,2.3\}\lambda'$, for $\beta=0.5$. All other experimental conditions are those of Fig. 4.